Dry sliding wear behaviour of Ti-TiB-TiN_x in-situ composite synthesised by reactive hot pressing

J.I. Silva and A.C. Alves

CMEMS-UMinho – Center for MicroElectroMechanical Systems,
Universidade do Minho,
Azurém, 4800-058 Guimarães, Portugal
Email: silvajoana52622@hotmail.com
Email: alexandra@dem.uminho.pt

A.M. Pinto, F.S. Silva and F. Toptan*

CMEMS-UMinho – Center for MicroElectroMechanical Systems,
Universidade do Minho,
Azurém, 4800-058 Guimarães, Portugal
and
Dept. Eng. Mecânica,
Universidade do Minho,
Azurém, 4800-058 Guimarães, Portugal
Fax: +351 253 516007
Email: anapinto@dem.uminho.pt
Email: fsamuel@dem.uminho.pt
Email: ftoptan@dem.uminho.pt
*Corresponding author

Abstract: Ti and its alloys are attractive materials for a variety of fields; however, a major problem of Ti and its alloys is their poor wear resistance. It is known that reinforcing Ti with hard ceramic phases can substantially improve the wear resistance. Thus, Ti-TiB-TiN_x in-situ metal matrix composites were synthesised by reactive hot pressing utilising Ti/BN powder blends with 23:1 Ti:BN weight ratio. Ball-on-plate reciprocating dry sliding wear tests were performed against a 10 mm of alumina ball under 10 N normal load, at a frequency of 1 Hz, and with the total stroke length of 3 mm during 1,800 s. Results showed that the total wear volume loss was significantly decreased on the composite ($11.4 \pm 2.0 \times 10^{-3}$ mm^3) as compared to the unreinforced Ti ($40.9 \pm 4.2 \times 10^{-3}$ mm^3) due to the strengthening effect of the in-situ reinforcing phases.

Keywords: in-situ composites; titanium; reactive hot pressing; wear.

Reference to this paper should be made as follows: Silva, J.I., Alves, A.C., Pinto, A.M., Silva, F.S. and Toptan, F. (2016) 'Dry sliding wear behaviour of Ti-TiB-TiN_x in-situ composite synthesised by reactive hot pressing', *Int. J. Surface Science and Engineering*, Vol. 10, No. 4, pp.317–329.

Biographical notes: J.I. Silva is a Materials Engineer. She received her Master's degree from Integrated Master Program on Materials Engineering, University of Minho, Guimarães, Portugal in 2014.

A.C. Alves is a PhD student at the Materials Science Program University of Minho. She received her Master's degree from Integrated Master Program on Materials Engineering, University of Minho in 2007.

A.M. Pinto is an Associated Professor at Department of Mechanical Engineering, Engineering School, University of Minho. She received her PhD on Metallurgical Engineering at Porto University in 1991. She is member of the research group on micro/nano technologies and smart systems of the Centre of MicroElectroMechanical Systems (CMEMS-UMinho) at University of Minho. Her research interests are focused on metallic and functionally graded materials exploring the following aspects: joining/bonding of intermetallics to similar and dissimilar materials (characterisation of bonding interfaces, study of bonding mechanisms) and development of functionally graded materials for biomedical applications (including in-situ composites, foams and surface modification).

F.S. Silva is a Full Professor at Department of Mechanical Engineering, Engineering School, University of Minho. He received his PhD on Mechanical Engineering at University of Minho in 2002. He is member of the research group on micro/nano technologies and smart systems of the Centre of MicroElectroMechanical Systems (CMEMS-UMinho) at University of Minho. His research interests are focused on fatigue and fracture of metal alloys and composite materials; processing and characterisation of functionally graded materials, shape memory alloys, and light-weight cellular materials, direct metal/ceramic multi-material laser sintering.

F. Toptan is an Assistant Professor at University of Minho, Mechanical Engineering Department. He received a BS degree in Metallurgical and Materials Engineering, MS and PhD degrees in Materials Science from Yildiz Technical University, Istanbul, Turkey. He is member of the research group on micro/nano technologies and smart systems of the Centre of MicroElectroMechanical Systems (CMEMS-UMinho) at University of Minho and IBTN/Br, Brazilian branch of the Institute of Biomaterials, Tribocorrosion and Nanomedicine. His research interests are focused on the development of metal matrix composites and investigation of the degradation mechanisms of those materials particularly due to wear, corrosion and tribocorrosion.

1 Introduction

Due to their properties such as high specific strength, long fatigue life, excellent corrosion resistance and biocompatibility, Ti and its alloys are attractive materials for a variety of fields including aerospace, chemical and biomedical industries (Li et al., 2013; Bolzoni et al., 2012; Rautray et al., 2011; Yap et al., 2011). However, a major problem of Ti and its alloys is their poor wear resistance. It is well known that incorporation of hard ceramic phases into a metal can result in a substantial improvement on the wear resistance (Kim et al., 2013, 2011; Doni et al., 2013; Qin et al., 2011; Attar et al., 2014). However, apart from mechanical and physical factors that involves the tribo-system, materials-related factors such as microstructure of the metallic matrix material; type, shape, size, volume fraction and distribution of the reinforcement; and particularly the properties of the matrix/reinforcement interface strongly influences the tribological performance of the metal matrix composites (MMCs) (Sannino and Rack, 1995; Shipway

et al., 1998; Rosenberger et al., 2005). In MMCs, if the interfacial bonding between the matrix and the reinforcement is not strong enough, the hard reinforcing phases can pull-out during sliding and can result in catastrophic wear by acting as extra abrasives (Qin et al., 2011; Toptan et al., 2013; Mondal and Das, 2006; Doni et al., 2014). Interface-related problems are known to be a major issue on ex-situ MMCs that arises mainly due to low wettability of matrix on the reinforcement phase, formation of detrimental reaction products at the interface and insufficient bonding between matrix and reinforcement (Ranganath, 1997; Toptan et al., 2013, 2010). On the other hand, in-situ composites, where reinforcing phases are synthesised during the processing, presents 'clean' interfaces, no detrimental reactions products, no interfacial discontinuities and usually stronger interfaces (Ranganath, 1997; Aikin, 1997).

Several studies were performed on in-situ composites utilising Ti together with reactants such as TiB_2, B_4C, B, C, and BN to form reinforcing phases such as TiB, TiB_2, TiC, TiN by using reactive sintering, reactive hot pressing, spark plasma sintering, self-propagating high-temperature synthesis, and liquid metallurgical routes (Radhakrishna Bhat et al., 2002; Kim et al., 2013, 2011; Feng et al., 2005; Atri et al., 1999; Chaudhari and Bauri, 2013; Wei et al., 2013; Panda and Chandran, 2003; Petukhov et al., 2007; Rangaraj et al., 2004; Yang et al., 2013; Yeh and Teng, 2006; Zhan et al., 2009; Contreras et al., 2004; Locci et al., 2006; Xinghong et al., 2002; Yeh and Chen, 2008; Zhang et al., 2013a; Gotman et al., 1998; Olevsky et al., 1996; Wang et al., 2012; Wen et al., 2001; Lu et al., 2002; Li et al., 2001, 2015; Qin et al., 2011; Das et al., 2014). Within this variety of combinations, Ti-B-N system has been studied by several authors (Rangaraj et al., 2004; Yang et al., 2013; Yeh and Teng, 2006; Olevsky et al., 1996; Li et al., 2001). Yang et al. (2013) presented a thermodynamic consideration on the Ti-BN system. The authors studied the potential reactions by taking consideration of the Ti-N and Ti-B phase diagrams and reported that TiN and TiB_2 are the most favourable reaction products in the Ti-BN system. However, it has been reported that in the presence of excess Ti, more specifically, if the average B concentration in the reaction zone is less than 18% in mass fraction, TiB_2 transforms to TiB at elevated temperatures (Chaudhari and Bauri, 2013; Zhang et al., 2013b).

In the literature, a numerous number of studies that are using Ti with several reactants to produce in-situ composites were aimed at development of ceramic matrix composites. Furthermore, most of the studies were focused on structural and microstructural characterisation of the in-situ composites while the studies on the wear behaviour are very limited. Qin et al. (2011) studied the dry sliding wear behaviour of TiB and TiC reinforced Ti−MMCs processed by reactive hot pressing followed by extrusion. After the dry sliding wear tests performed against a tool steel counter material by using a pin-on-disk tribometer, the authors reported that in-situ ceramic phases significantly improved the wear resistance of pure Ti as well resulted in lower coefficient of friction (COF). The similar system (Ti-TiB-TiC) produced by lost-wax method was also tested by Kim et al. (2011) against a 52100 bearing steel ball by using a ball-on-disk tribometer, where lower wear loss and COF values were also reported. Kim et al. (2013) recently studied the fretting behaviour of Ti-TiB-TiC MMCs against a bearing steel ball specimen and reported that the wear volume loss decreased with the increased volume fraction of the hard ceramic phases.

Combination of the reinforcing phases of TiB and TiN also offers to improve the wear resistance of Ti owing to their high hardness, excellent thermal and chemical stability and corrosion resistance (Tomoshige et al., 1997; Wei et al., 2013; Sahay et al.,

2011). However, the wear behaviour of in-situ Ti-TiB-TiN MMCs is yet to be studied. Thus, the present work aimed at studying the dry sliding wear behaviour of Ti-TiB-TiN_x in-situ MMCs synthesized by reactive hot pressing.

2 Experimental procedure

In-situ Ti-TiB-TiN_x composites were synthesised by using Ti and BN particles having 28.8 and 1 μm average particle sizes, respectively. Particle blends having 23:1 Ti:BN weight ratio were ball milled at 25 rpm speed during 3h using alumina balls. Prior to the processing, powder mixture was dried in a muffle furnace at 105°C for 1 h in order to remove the humidity.

For the reactive hot pressing process, the powder mixtures were inserted into a zirconia painted graphite die having 10 mm diameter. The graphite die was mounted in to a hydraulic press and heated up to 1,100°C with a heating rate of 12°C/min, using an induction furnace. The entire process was performed under 10^{-2} mbar vacuum and 40 MPa constant pressure with a sintering time of 30 min. Unreinforced Ti samples were also processed following the same processing route to be used as control group.

After processing, the samples were grinded and polished using SiC papers and colloidal silica suspensions down to 0.04 μm. After polishing, samples were ultrasonically cleaned in propanol for 10 min followed by distilled water during 5 min. Phase analysis of the as-processed in-situ composites was carried out by X-ray diffraction (XRD) using a Bruker D8 Discover diffractometer equipped with a Cu Kα radiation source. In order to characterise the in-situ reinforcing phases, composite samples were deeply-etched by Kroll's reagent ($HF:HNO_3:H_2O$) and the microstructures were investigated by FEI Quanta 400 Field emission gun scanning electron microscope (FEG-SEM) equipped with EDAX Genesis X4M energy dispersive X-ray spectroscopy (EDS) and FEI Nova 200 FEG-SEM equipped with EDAX EDS. Vickers hardness was evaluated by using Officine Galileo Mod. D 200 tester by a mean of five indentations per sample with 30 kg load and 20 s dwelling time.

Dry sliding wear tests were performed on a tribometer (CETR-UMT-2) using ball-on-plate configuration with a reciprocating plate adapter. An alumina ball of 10 mm diameter (Ceratec) was used as a static counter material and the samples were placed as the moving body. The tests were performed in ambient air (24 ± 2°C), under 10 N normal load, at a frequency of 1 Hz, and with the total stroke length of 3 mm during 1,800 s. Tests were repeated at least three times in order to assure the repeatability.

After the tests, wear debris were collected and the samples were cleaned following the procedure applied after metallographic sample preparation. Worn surfaces and wear debris were characterised using FEI Nova 200 FEG-SEM equipped with EDAX EDS (all worn surface micrographs were taken as parallel to the sliding direction). Besides, 2D profiles were obtained from the wear tracks by a contact profilometer (Mitutoyo Surtest SJ-500) and the total wear volume loss values were calculated following the procedure given elsewhere (Doni et al., 2013).

3 Results and discussion

Li et al. (2001) investigated the microstructure evolution on Ti/BN powder blends having 3:2 Ti to BN molar ratio and reported after DSC analysis that TiN phase forms between 300−500°C, whereas TiB_2 and TiB phases form at the temperature range of 500−900°C. On the other hand, as stated above, in the presence of excess Ti, TiB_2 transforms to TiB at elevated temperatures (Chaudhari and Bauri, 2013; Zhang et al., 2013b). Furthermore, Yang et al. (2013) reported for the Ti-BN system that N atoms dissolve into the α-Ti as interstitials and form α-$TiN_{0.3}$. Then, N atoms from BN react with α-$TiN_{0.3}$ and form Ti_2N and sub-stoichiometric TiN_x. Above 1,100°C, Ti_2N transforms to TiN_x where as more N atoms diffuse into the TiN_x phase, its composition becomes close to stoichiometric TiN. As can be seen on the XRD spectrum given in Figure 1(a), the composites exhibited TiB and TiN_x in-situ reinforcement phases, as in accordance with the literature. On the other hand, it is known that B atoms have faster diffusion rates in the [010] direction as compared to the other directions, resulting in a needle-like morphology for the TiB phase (Quast et al., 2008; Sahay et al., 2011). The TiB whiskers were not clearly visible on the polished as-processed surfaces [Figure 1(b)], while they were clearly observed on the SEM images of the deep-etched composite samples [Figure 1(c)] as in accordance with the literature (Zhang et al., 2013b; Wei et al., 2013). However, although TiN_x phase was detected by XRD and the presence of N was found by EDS [Figure 1(c)], TiN_x phase was not visible on the SEM images probably due to its finer structure (Li et al., 2001). Thus, further characterisation studies (i.e., TEM) are needed for microstructural characterisation of TiN_x phase.

Figure 1 (a) XRD spectrum of the composite sample (b) Backscattered electron image of the as-processed composite (c) Secondary electron image of deep-etched composite sample together with EDS spectra taken from the marked zones (see online version for colours)

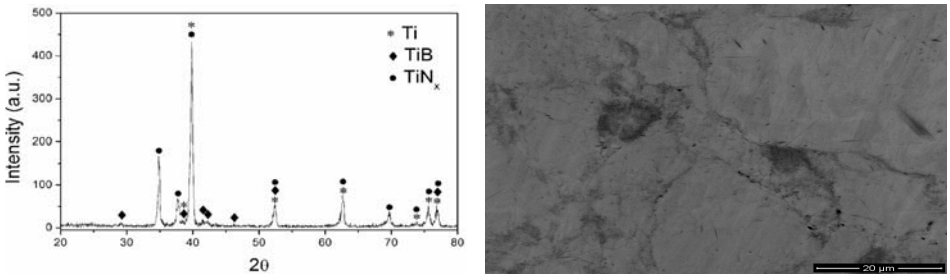

(a) (b)

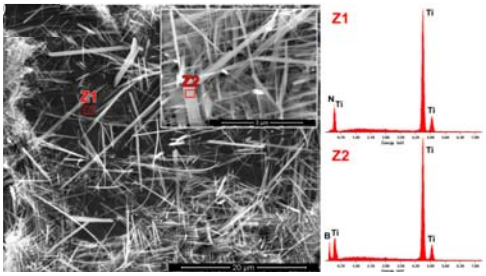

(c)

Figure 2 Low magnification se and BSE images of the wear tracks from (a) unreinforced and (b) composite samples; higher magnification se and BSE images taken from inside of the wear tracks of (c) unreinforced and d) composite samples; detailed BSE images taken from the marked zones on c and d showing (e) oxide patches on the unreinforced sample and (f) compacted wear debris on the composite sample

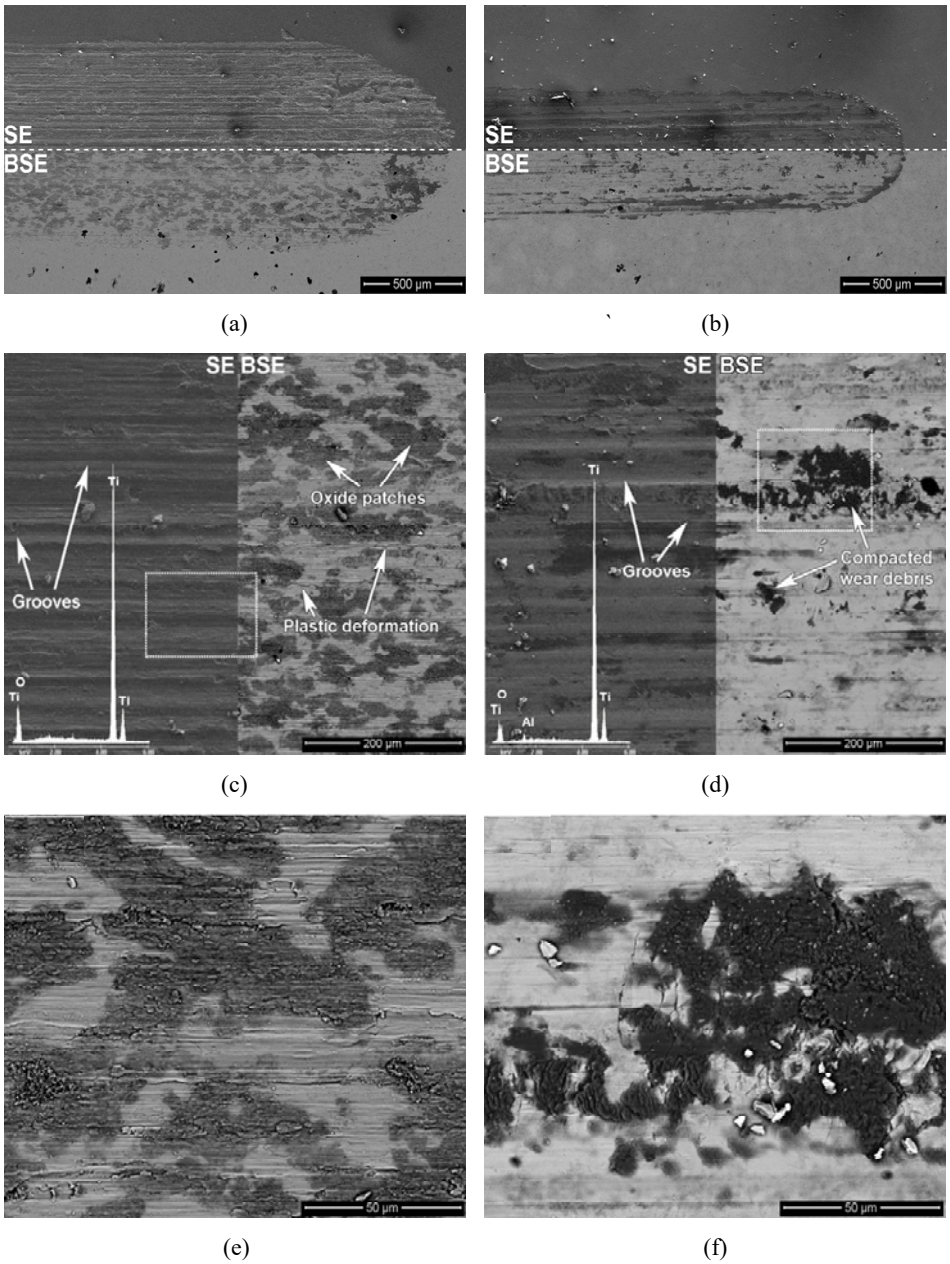

Figures 2(a) and 2(b) gives the representative low magnification SEM images of the wear tracks. As can be seen on the images, composite samples presented thinner wear tracks as compared to the unreinforced samples. Besides, parallel sliding grooves and

tribochemical features can also be seen on the images presented in secondary electron (SE) and backscattered electron (BSE) modes, respectively. The topography and the features can be seen more clearly on the higher magnification images taken from the wear tracks given in Figures 2(c)−2(f), together with the representative EDS spectra taken from the wear track areas, revealing the presence of oxides.

Titanium oxides may form on the worn surfaces due to the repetitive material transfer between the sliding surfaces resulting in formation of adhered/mixed oxide patches (Zivic et al., 2011; Dong and Bell, 1999; Doni et al., 2013). Oxidational wear describes a wear mechanism where oxide films are formed at the contact area due to the elevated temperature at the sliding zone. It is known that these oxides can play a protective role during sliding of metallic materials. However, when the oxide layers reach a critical thickness, they can break up resulting in formation of oxide wear debris (Srinivasan et al., 2002; Zafari et al., 2012; Quinn, 1983; Yap et al., 2011). As can be seen on Figures 2(a), 2(c), and 2(e), although the oxide patches covered a relatively higher area fraction on the worn surfaces, it was not a continuous layer, thus, could not completely avoid the contact of the counter material with the Ti surface, resulting in grooves on the worn surfaces [Figures 2(c) and 2(e)]. Worn composite surfaces, on the other hand, exhibited relatively compact wear debris with a smaller area fraction as compared to the oxide patches on the unreinforced sample surfaces. In addition to oxygen, EDS analysis also revealed the presence of Al pointing a considerable amount of material transfer from the counter material (alumina ball).

Figure 3 SE images of the counter material surfaces worn against (a) unreinforced and (b) composite samples, together with EDS spectra of the wear scars (see online version for colours)

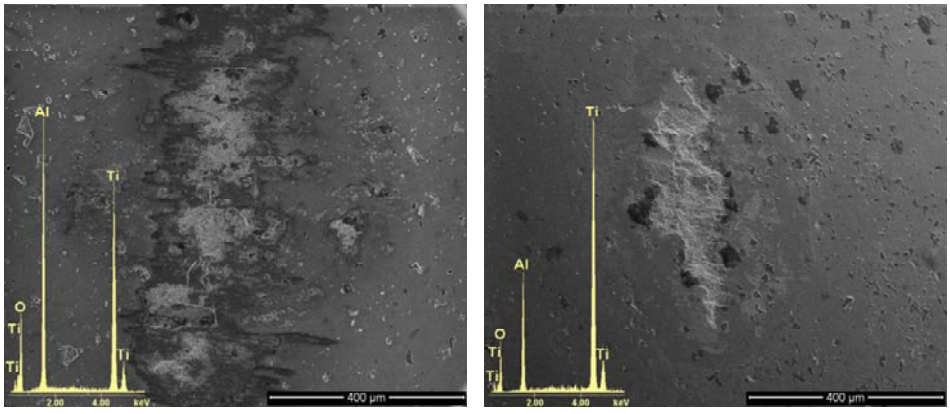

(a) (b)

Figures 3(a) and 3(b) present the SE images of the worn counter material surfaces together with EDS spectra taken from the wear scars. Material transfer from the samples to the alumina ball surfaces were detected on both samples. The wear scars on the balls corresponding to the unreinforced samples were bigger whereas the dominant feature was observed as adhesion of titanium. However, although no profilometric study was performed on the worn alumina surfaces, SEM images suggested more wear damage on the balls corresponding to the composite samples resulting in transfer of alumina debris to the composite surfaces [Figure 2(d)].

Figure 4 Evolution of the COF during dry sliding (see online version for colours)

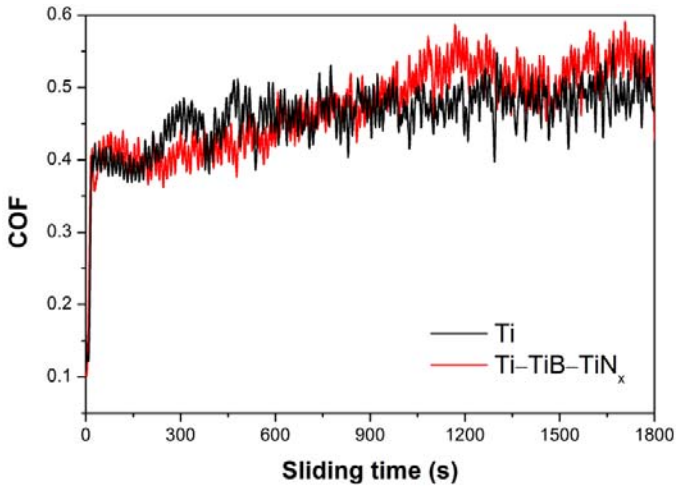

The representative evolution of COF during sliding is given in Figure 4. As soon as sliding started, COF values were suddenly reached the values around 0.4 for both materials. The values for the unreinforced titanium first slightly decreased then gradually increased up to approx. 0.48 at around 300 s and after this point, oscillated around this value till the end of the sliding. A slight decrease at the beginnings of the sliding was also observed for the composite samples. Then, the values were gradually increased up to approx. 0.53 around 1,100 s. After this point, the values presented waves and oscillations around this value.

Figure 5 BSE images of the wear debris obtained from (a) unreinforced and (b) composite sample (see online version for colours)

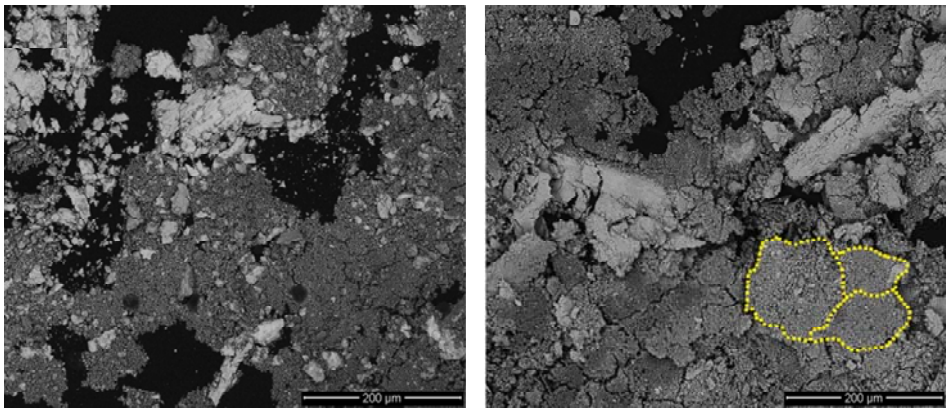

(a) (b)

The evolution of the COF values during approx. first 300 s for the unreinforced samples may be attributed to the oxide patches. At the first half of this period, the slight decrease on the values can be related to the formation of the patches resulting in decreased metal/oxide contact and increased oxide/oxide contact. However, since the oxide patches

formed discontinuously, as the thickness of the patches increased, the roughness of the worn surface may increase, leading to increased COF values between approx. 150 and 300 s of sliding. After this point, the patches may be reached to a certain thickness and may be broken by the counter material leading to the formation of fine oxide debris [Figure 5(a)]. The entrapped debris on the sliding zone (i.e., third body particles) can lead to oscillations on the COF values (Doni et al., 2013). The evolution of COF on the composite sample presented relatively similar behaviour during approx. first 150 s of sliding. The gradual increase on the values after this point can be related to the formation of the compacted wear debris. SEM images of the wear debris (Figure 5) suggested that unreinforced titanium generated loose, fine wear debris, whereas the debris on the composite samples exhibited compacted, flake-like shape [flakes indicated with dashed lines on Figure 5(b)]. Relatively higher COF values on the composite samples during approx. last 700 s of sliding may be attributed to roughened surface by the formation of the compacted wear debris as well formation of the third body particles. Furthermore, wear debris on the composite samples may be harder due to presence of the reinforcing phases as well as alumina debris transferred from the counter material [Figure 2(d)] contributing in slightly higher COF values during the last period of the sliding.

Figure 6 Representative wear track profiles (see online version for colours)

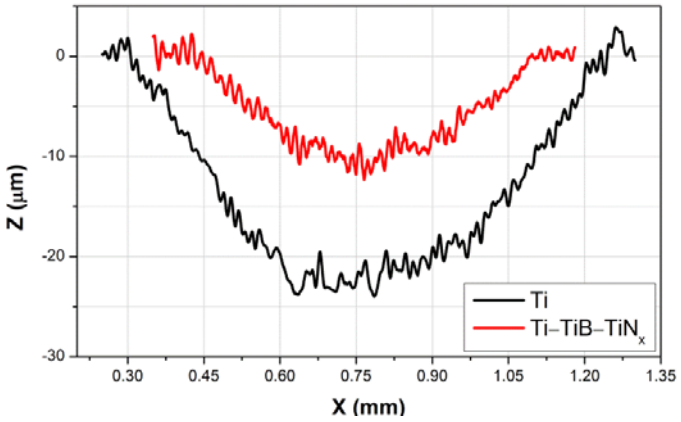

After microstructural and chemical analysis of the mating surfaces and wear debris, together with the analysis of the COF evolution during the sliding, it is deduced that wear mechanism for the unreinforced sample was mainly a combination of abrasive, adhesive, and oxidative wear, whereas composite samples exhibited mainly abrasive wear. Increased hardness of the composite samples due to the in-situ nano/micro reinforcements resulted in a significant increase on the hardness (316 ± 27 and 736 ± 65 HV for the unreinforced and composite samples, respectively) leading to less plastic deformation on the composite samples. It is known that strengthening can take place on MMCs by direct and indirect strengthening. Direct strengthening in discontinuously reinforced MMCs is considered as an extension of the classical composite strengthening mechanisms where under an applied load, the load is transferred from matrix to the reinforcement through the interface. Thus, if the matrix/reinforcement interface is strong, strengthening takes place by the contribution of the reinforcing phase on carrying of the load. Besides, reinforcing phases can lead to dislocations that can be generated either by

straining in response to an applied load or straining due to the coefficient of thermal expansion (CTE) mismatch between matrix and reinforcement, or dislocation motion can be impeded by the reinforcing phase on a matrix slip plane that is known as indirect strengthening (Chawla and Shen, 2001; Russell and Lee, 2005). As a result, the total wear volume loss was significantly decreased on the composite samples ($11.4 \pm 2.0 \times 10^{-3}$ mm^3) as compared to the unreinforced samples ($40.9 \pm 4.2 \times 10^{-3}$ mm^3), which can also be seen clearly on the representative wear profiles given in Figure 6.

4 Conclusions

Reciprocal dry sliding wear behaviour of Ti-TiB-TiN_x in-situ composites synthesised by reactive hot pressing using Ti/BN powder blends with 23:1 Ti:BN weight ratio was studied. The reactive hot pressing at 1,100°C resulted in in-situ formation of TiB and TiN_x phases that increased the hardness from 316 ± 27 to 736 ± 65 HV. Owing to the strengthening effect given by the in-situ reinforcing phases, total wear volume loss was significantly decreased on the composite samples ($11.4 \pm 2.0 \times 10^{-3}$ mm^3) as compared to the unreinforced samples ($40.9 \pm 4.2 \times 10^{-3}$ mm^3). While the unreinforced Ti exhibited mainly a combination of abrasive, adhesive, and oxidative wear, abrasive wear was the dominant mechanism for the in-situ composite. These results suggested that Ti-TiB-TiN_x in-situ composites can find some applications where lower wear resistance of titanium is problematic. However, further studies are needed in order to have a deeper understanding to the wear behaviour of these in-situ composites as a function of volume fraction of the in-situ phases and testing parameters (normal load, sliding frequency, sliding time, etc). Furthermore, since several applications are being exposed to corrosive environments, tribocorrosion behaviour of these composites also needs to be studied.

Acknowledgements

This study was supported by The Calouste Gulbenkian Foundation through *Programa de Mobilidade Académica para Professores* and Portuguese Foundation for Science and Technology (FCT-Portugal), under the project EXCL/EMS-TEC/0460/2012. The authors also would like to thank Prof. Amílcar Ramalho (Universidade de Coimbra) for the provision of profilometry facilities.

References

Aikin, R.M. (1997) 'The mechanical properties of in-situ composites', *JOM*, Vol. 49, No. 8, pp.35–39.

Atri, R.R., Ravichandran, K.S. and Jha, S.K. (1999) 'Elastic properties of in-situ processed Ti-TiB composites measured by impulse excitation of vibration', *Materials Science and Engineering: A*, Vol. 271, Nos. 1–2, pp.150–159.

Attar, H. et al. (2014) 'Selective laser melting of in situ titanium-titanium boride composites: processing, microstructure and mechanical properties', *Acta Materialia*, 1 September, Vol. 76, pp.13–22.

Bolzoni, L. et al. (2012) 'Inductive hot-pressing of titanium and titanium alloy powders', *Materials Chemistry and Physics*, Vol. 131, No. 3, pp.672–679.

Chaudhari, R. and Bauri, R. (2013) 'Reaction mechanism, microstructure and properties of Ti-TiB insitu composite processed by spark plasma sintering', *Materials Science & Engineering A*, 10 December, Vol. 587, pp.161–167.

Chawla, N. and Shen, Y-L. (2001) 'Mechanical behavior of particle reinforced metal matrix composites', *Advanced Engineering Materials*, Vol. 3, No. 6, pp.357–370.

Contreras, L. et al. (2004) 'Time-resolved XRD study of TiC–TiB2 composites obtained by SHS', *Acta Materialia*, Vol. 52, No. 16, pp.4783–4790..

Das, M. et al. (2014) 'In situ synthesized TiB-TiN reinforced Ti6Al4V alloy composite coatings: microstructure, tribological and in-vitro biocompatibility', *Journal of the Mechanical Behavior of Biomedical Materials*, January, Vol. 29, pp.259–71.

Dong, H. and Bell, T. (1999) 'Tribological behaviour of alumina sliding against Ti6Al4V in unlubricated contact', *Wear*, April, Vols. 225–229, Part 2, pp.874–884.

Doni, Z. et al. (2013) 'Dry sliding and tribocorrosion behaviour of hot pressed CoCrMo biomedical alloy as compared with the cast CoCrMo and Ti6Al4V alloys', *Materials & Design*, December, Vol. 52, pp.47–57.

Doni, Z. et al. (2014) 'Tribocorrosion behaviour of hot pressed CoCrMo−Al2O3 composites for biomedical applications', *Tribology – Materials, Surfaces & Interfaces*, Vol. 8, No. 4, pp.201–208.

Feng, H. et al. (2005) 'Spark plasma sintering of functionally graded material in the Ti-TiB2-B system', *Materials Science and Engineering: A*, Vol. 397, Nos. 1–2, pp.92–97.

Gotman, I., Travitzky, N.A. and Gutmanas, E.Y. (1998) 'Dense in situ TiB2/TiN and TiB2/TiC ceramic matrix composites: reactive synthesis and properties', *Materials Science and Engineering A*, March, Vol. 244, No. 1, pp.127–137.

Kim, I.Y. et al. (2011) 'Friction and wear behavior of titanium matrix (TiB+TiC) composites', *Wear*, Vol. 271, Nos. 9–10, pp.1962–1965.

Kim, J-S. et al. (2013) 'Fretting wear characteristics of titanium matrix composites reinforced by titanium boride and titanium carbide particulates', *Wear*, Vol. 301, Nos. 1–2, pp.562–568.

Li, J., Hu, K. and Zhong, Y. (2001) 'Microstructure evolution of Ti/BN powder blend during ball milling and heat treatment', *J. Mater. Sci. Technol.*, Vol. 17, No. 1, pp.s101–s104.

Li, S. et al. (2013) 'Powder metallurgy titanium metal matrix composites reinforced with carbon nanotubes and graphite', *Composites Part A: Applied Science and Manufacturing*, May, Vol. 48, pp.57–66.

Li, S. et al. (2015) 'Microstructure and mechanical properties of P/M titanium matrix composites reinforced by in-situ synthesized TiC–TiB', *Materials Science and Engineering: A*, March, Vol. 628, pp.75–83.

Locci, A.M. et al. (2006) 'Simultaneous spark plasma synthesis and densification of TiC-TiB2 composites', *Journal of the American Ceramic Society*, Vol. 89, No. 3, pp.848–855.

Lu, W.J. et al. (2002) 'Solidification paths and reinforcement morphologies in melt-processed (TiB + TiC)/Ti in situ composites', *Metallurgical and Materials Transactions A*, Vol. 33A, No. 9, pp.3055–3063.

Mondal, D.P. and Das, S. (2006) 'High stress abrasive wear behaviour of aluminium hard particle composites: effect of experimental parameters, particle size and volume fraction', *Tribology International*, Vol. 39, No. 6, pp.470–478.

Olevsky, F. et al. (1996) 'Synthesis of in situ TiB2/TiN ceramic matrix composites from dense BN-Ti and BN-Ti-Ni powder blends', *Metallurgical and Materials Transactions A*, Vol. 27A, No. 8, pp.2071–2079.

Panda, K.B. and Chandran, K.S.R. (2003) 'Titanium-titanium boride (Ti-TiB) functionally graded materials through reaction sintering: synthesis, microstructure, and properties', *Metallurgical and Materials Transactions A*, Vol. 34, No. 9, pp.1993–2003.

Petukhov, A.S. et al. (2007) 'Reactive electric-discharge sintering of TiN-TiB2', *Powder Metallurgy and Metal Ceramics*, Vol. 46, Nos. 11–12, pp.525–532.

Qin, Y., Geng, L. and Ni, D. (2011) 'Dry sliding wear behavior of extruded titanium matrix composite reinforced by in situ TiB whisker and TiC particle', *Journal of Materials Science*, Vol. 46, No. 14, pp.4980–4985.

Quast, J.P. et al. (2008) 'A microstructure and sonic fatigue investigation of Ti-TiB functionally graded materials', *Materials Science and Engineering: A*, Vol. 497, Nos. 1–2, pp.1–9.

Quinn, T.F.J. (1983) 'Review of oxidational wear: part I: the origins of oxidational wear', *Tribology International*, Vol. 16, No. 5, pp.257–271.

Radhakrishna Bhat, B.V., Subramanyam, J. and Bhanu Prasad, V.V. (2002) 'Preparation of Ti-TiB-TiC & Ti-TiB composites by in-situ reaction hot pressing', *Materials Science and Engineering: A*, Vol. 325, No. 1–2, pp.126–130.

Ranganath, S. (1997) 'A review on particulate-reinforced titanium matrix composites', *Journal of Materials Science*, Vol. 32, No. 1, pp.1–16.

Rangaraj, L., Divakar, C. and Jayaram, V. (2004) 'Reactive hot pressing of titanium nitride – titanium diboride composites at moderate pressures and temperatures', *J. Am. Ceram. Soc.*, Vol. 87, No. 10, pp.1872–1878.

Rautray, T.R., Narayanan, R. and Kim, K-H. (2011) 'Ion implantation of titanium based biomaterials', *Progress in Materials Science*, Vol. 56, No. 8, pp.1137–1177.

Rosenberger, M.R., Schvezov, C.E. and Forlerer, E. (2005) 'Wear of different aluminum matrix composites under conditions that generate a mechanically mixed layer', *Wear*, Vol. 259, Nos. 1–6, pp.590–601.

Russell, A.M. and Lee, K.L. (2005) *Structure Property Relations in Nonferrous Metals*, John Wiley & Sons, Inc, New Jersey.

Sahay, S.S. et al. (2011) 'Evolution of microstructure and phases in in situ processed Ti-TiB composites containing high volume fractions of TiB whiskers', *Journal of Materials Research*, Vol. 14, No. 11, pp.4214–4223.

Sannino, A.P. and Rack, H.J. (1995) 'Dry sliding wear of discontinuously reinforced aluminum composites: review and discussion', *Wear*, Vol. 189, Nos. 1–2, pp.1–19.

Shipway, P.H., Kennedy, A.R. and Wilkes, A.J. (1998) 'Sliding wear behaviour of aluminium-based metal matrix composites produced by a novel liquid route', *Wear*, Vol. 216, No. 2, pp.160–171.

Srinivasan, P.B., Krishnakumar, C. V. and Krishnaraj, N. (2002) 'Sliding wear behavior of salt bath nitrocarburized medium carbon steel', *Journal of Materials Engineering and Performance*, Vol. 11, No. 5, pp.509–515.

Tomoshige, R., Murayama, A. and Matsushita, T. (1997) 'Production of TiB2-TiN composites by combustion synthesis and their properties', *Journal of American Ceramic Society*, Vol. 80, No. 3, pp.761–764.

Toptan, F. et al. (2013) 'Corrosion and tribocorrosion behaviour of Al-Si-Cu-Mg alloy and its composites reinforced with B4C particles in 0.05M NaCl solution', *Wear*, Vol. 306, Nos. 1–2, pp.27–35.

Toptan, F., Kilicarslan, A. and Kerti, I. (2010) 'The effect of Ti addition on the properties of Al-B4C interface: a microstructural study', *Materials Science Forum*, Vols. 636–637, pp.192–197.

Wang, H. et al. (2012) 'Characterization of the structure of TiB2/TiC composites prepared via mechanical alloying and subsequent pressureless sintering', *Powder Technology*, February, Vol. 217, pp.340–346.

Wei, S. et al. (2013) 'Effect of Ti content and sintering temperature on the microstructures and mechanical properties of TiB reinforced titanium composites synthesized by SPS process', *Materials Science and Engineering: A*, 10 January, Vol. 560, pp.249–255.

Wen, G. et al. (2001) 'Reaction synthesis of TiB2-TiC composites with enhanced toughness', *Acta Materialia*, Vol. 49, No. 8, pp.1463–1470.

Xinghong, Z. et al. (2002) 'Self-propagating high temperature combustion synthesis of TiC/TiB2 ceramic-matrix composites', *Composites Science and Technology*, Vol. 62, No. 15, pp.2037–2041.

Yang, Z-L. et al. (2013) 'Synthesis route and mechanical properties of reactive hot pressed TiN-TiB2 ceramics', *International Journal of Refractory Metals and Hard Materials*, November, Vol. 41, pp.54–59.

Yap, T.C. et al. (2011) 'Correlation of wear debris morphology and wear mechanism of Ti-5Al-4V-0.6Mo-0.4Fe slides against tungsten carbide under dry and cryogenic conditions', *International Journal of Surface Science and Engineering*, Vol. 5, Nos. 5/6, p.463.

Yeh, C.L. and Chen, Y.L. (2008) 'Combustion synthesis of TiC–TiB2 composites', *Journal of Alloys and Compounds*, Vol. 463, Nos. 1–2, pp.373–377.

Yeh, C.L. and Teng, G.S. (2006) 'Combustion synthesis of TiN-TiB2 composites in Ti/BN/N2 and Ti/BN/B reaction systems', *Journal of Alloys and Compounds*, Vol. 424, Nos. 1–2, pp.152–158.

Zafari, A., Ghasemi, H.M. and Mahmudi, R. (2012) 'Tribological behavior of AZ91D magnesium alloy at elevated temperatures', *Wear*, 15 July, Vols. 292–293, pp.33–40.

Zhan, L. et al. (2009) 'Self-propagating high-temperature synthesis of TiCxNy-TiB2 ceramics from a Ti-B4C-BN system', *International Journal of Refractory Metals and Hard Materials*, Vol. 27, No. 5, pp.829–834.

Zhang, Z. et al. (2013a) 'A new rapid route to in-situ synthesize TiB-Ti system functionally graded materials using spark plasma sintering method', *Materials Science & Engineering A*, 10 March, Vol. 565, pp.326–332.

Zhang, Z. et al. (2013b) 'Microstructure characteristics and mechanical properties of TiB/Ti-1.5Fe-2.25Mo composites synthesized in situ using SPS process', *Transactions of Nonferrous Metals Society of China*, Vol. 23, No. 9, pp.2598–2604.

Zivic, F., Babic, M. and Vencl, A. (2011) 'Continuous control as alternative route for wear monitoring by measuring penetration depth during linear reciprocating sliding of Ti6Al4V alloy', *Journal of Alloys and Compounds*, Vol. 509, No. 19, pp.5748–5754.